hep-ph 1009.3801

arXiv:1009.3801v1 [hep-ph] 20 Sep 2010

CERN-PH-TH/2010-203; MCTP-10-41; IFT-10-11; DESY 10-143

Supersymmetric mass spectra for gravitino dark matter with a high reheating temperature

L. Covi[a], M. Olechowski[b], S. Pokorski[b] *,
K. Turzyński[b], J. D. Wells[c,d]

[a] *Deutsches Elektronen-Synchrotron, DESY, Hamburg, Germany*
[b] *Institute of Theoretical Physics, University of Warsaw, Hoża 69, 00-681, Warsaw, Poland*
[c] *CERN Theory Group (PH-TH), CH-1211 Geneva 23, Switzerland*
[d] *MCTP, University of Michigan, Ann Arbor, MI 48109, USA*

Supersymmetric theories with gravitino dark matter generally do not allow the high reheating temperature required by thermal leptogenesis without running afoul of relic abundance or big bang nucleosynthesis constraints. We report on a successful search for parameter space that does satisfy these requirements. The main implication is the near degeneracy of the gluino with the other neutralinos in the spectrum. The leading discovery channel at the LHC for this scenario is through monojet plus missing energy events.

I. GRAVITINOS FROM HIGH REHEATING TEMPERATURE

Our goal is to investigate the supersymmetry spectrum that allows gravitinos to be the lightest supersymmetric partner (LSP) dark matter of the universe and also allows thermal leptogenesis to explain the baryon asymmetry, all while retaining the successful predictions of big bang nucleosynthesis. We explain each of these in turn, highlighting the potential sources of conflict between them, and finally settling upon an explanation requiring a neutralino next-to-lightest supersymmetric partner (NLSP) degenerate with the gluino, and then investigating its consequences for the Large Hadron Collider (LHC).

To begin we note that in gauge mediated supersymmetry [1] the lightest supersymmetric particle (LSP) is generically the gravitino, with mass ranging from the eV scale to tens of GeV. There are many nice features of this model that we do not detail here, but suffice it to say that it is a powerful and viable organizing principle for the superpartner spectrum, and motivates our interest in the gravitino as the LSP. The identity of the next to lightest supersymmetric particle and the details of the spectrum are model dependent (see *e.g.*, [2]). Being the LSP and stable, the gravitino is the leading candidate for dark matter in these models, apart from the possibility of very long-lived particles in the messenger sector [3]. However, a light gravitino is at most Warm Dark Matter and not favoured by structure formation; indeed, present observations already constrain its mass to be above a few keV if it decouples as a relativistic thermal relic [4].

This is not the only source of gravitinos in the early Universe, as they do not have to reach thermal equilibrium densities to be cosmologically important. On one hand, scatterings in the thermal plasma produce gravitinos with the abundance proportional to the reheating temperature after inflation [5–7]:

$$\Omega_{\tilde{G}}^{\rm TP} h^2 \approx \frac{\left(\frac{T_{\rm R}}{10^9\,{\rm GeV}}\right)\left(\frac{m_{\rm NLSP}}{300\,{\rm GeV}}\right)^2}{\left(\frac{m_{3/2}}{1\,{\rm GeV}}\right)} \sum_r \gamma_r \cdot \left(\frac{M_r}{m_{\rm NLSP}}\right)^2 , \quad (1)$$

where M_r denote physical gaugino masses and the coefficients γ_r depend on the ratios of the gauge couplings at the reheating scale and the scale of the physical gaugino masses: with the 1-loop RGE for the gaugino masses, the values of γ_r can be evaluated for $T_{\rm R} = 10^9\,(10^7)\,{\rm GeV}$ as $\gamma_3 = 0.48 - 0.56\,(0.62 - 0.74)$, $\gamma_2 = 0.57\,(0.54)$, $\gamma_1 = 0.22\,(0.17)$, where the range for γ_3 corresponds to the gluino masses ranging from 200 to 900 GeV [8]. We have only included the production of the goldstino component of the gravitino, which dominates for $m_{\rm NLSP}/m_{3/2} > \mathcal{O}(10)$. On the other hand, gravitinos are also produced in the gravitational decays of the NLSP, but for $\Omega_{\rm NLSP}h^2 \ll 1$ or $m_{3/2}/m_{\rm NLSP} \ll 1$ these decays are a negligible source of gravitino dark matter; moreover, too high a fraction of such a nonthermal and warmish dark matter component can cause too much erasure of the cosmic structures at small scales [9]. Other contributions to the gravitino abundance can arise from inflaton decay [10] or from the reheating process [11], but they are more model dependent and we will not discuss them further.

Thus, the gravitino abundance is largely determined directly by the reheating temperature $\Omega_{\tilde{G}} \sim T_R$, as suggested by eq. (1). If this were the only way the reheating temperature affected the scenario, one could contemplate a simple explanation for the cold dark matter by tuning T_R to achieve the required $\Omega_{\tilde{G}}$.

However, there are other implications to the choice of T_R that must be considered. Thermal leptogenesis requires a rather high T_R to be successful, which may yield too much dark matter unless the gravitino mass is lifted to higher values ($\Omega_{\tilde{G}} \sim T_R/m_{3/2}$, assuming $m_{\rm NLSP}$ is fixed). However, higher gravitino mass means a slower

*Hans Fischer Senior Fellow, Institute for Advanced Studies, Technical University, Munich, Germany

NLSP decay, which follows a normal thermal relic history and then dumps its decay energy into NLSP $\to \tilde{G}+X$ after big bang nucleosynthesis (BBN). BBN compatibility depends on both the number density of the NLSP $n_{\rm NLSP}$ and its decay lifetime $\tau_{\rm NLSP}$ and other quantities (such as the decay branching fractions, the gravitino mass, etc.). Thus, there are strains and potential incompatibilities when requiring compatibility among gravitino dark matter, thermal leptogenesis and big bang nucleosynthesis.

In the next two subsections we shall describe in more detail the constraints that arise from requiring both successful thermal leptogenesis and compatibility with BBN. We shall then explain in sec. I C our emphasis on scenarios with neutralino NLSP. In sec. II we determine the maximum allowed reheating temperature, which is wanted by thermal leptogenesis, consistent with all the constraints. We show how this value depends on other parameters of the theory. In sec. III we discuss the implications of the resulting parameter space for the Tevatron and Large Hadron Collider. We summarize our conclusions in sec. IV and make some additional final remarks.

A. Thermal Leptogenesis Requirements

Generation of the baryon asymmetry through thermal leptogenesis remains a theoretically attractive and experimentally viable possibility, as it only uses particles (right-handed neutrinos) and interactions (neutrino Yukawa couplings) already present in the seesaw models explaining the smallness of the neutrino masses (for a review, see [12]). Putting it simply, the lepton asymmetries, subsequently converted into baryon asymmetry, are produced in the CP violating decays of the lightest right-handed neutrinos; it is usually assumed that these neutrinos had been previously produced in scatterings in the thermal plasma. So successful thermal leptogenesis gives a lower bound on the mass of the lightest neutrino, $M_{N_1}^{(\rm min)}$, in usual seesaw models (with hierarchical masses of the right-handed neutrinos), which can be translated into a lower bound on the reheating temperature after inflation: $T_R^{(\rm min)} \approx M_{N_1}^{(\rm min)}/5$ ($T_R^{(\rm min)} \approx M_{N_1}^{(\rm min)}$) in the so-called strong (weak) washout regime.

Interestingly, the lower bound $T_R^{(\rm min)} = 1.9 \cdot 10^9\,{\rm GeV}$ [13] found in the model with the largest possible CP asymmetries and optimal (small) washout approximately coincides with values of T_R obtained in generic models predicting the correct baryon asymmetry, found with the Monte Carlo Markov chain techniques [14]. However, this bound on the reheating temperature is not an absolute one. If the initial conditions for leptogenesis include a thermal distribution of the lightest right-handed neutrino, the minimal reheating temperature is $2.5 \cdot 10^8\,{\rm GeV}$ [15]. This is the uncomfortably high reheating temperature with respect to gravitino abundance that we referred to above in the introduction. Such a high T_R puts strain on a light gravitino LSP being the dark matter while being consistent with BBN, even if one tries to make it as large as possible by requiring that the masses of the gauginos and the NLSP are not too far apart [8]. That consistency is the subject of the next subsection.

Before closing this discussion, we remark on a few caveats to what was said above. It has been argued that neglecting quantum effects in the dynamics of leptogenesis introduces theoretical uncertainties as large as an order of magnitude [16]. Furthermore, the bounds discussed above do not apply in models with degenerate masses of the right handed neutrinos, see *e.g.*, [17, 18], or in models with large cancellations in the seesaw mass formula [19, 20]. However, these solutions are of somewhat less interest to us here since they involve a degree and type of fine tuning that we wish to try to avoid. We also note that the reheating temperature may be lowered in models of nonthermal leptogenesis, see *e.g.*, [21, 22], or in soft leptogenesis, see [23–25]. Such models, however, require arranging for additional interactions, *e.g.* a coupling between the inflaton and a right-handed neutrino or a coupling of the Higgs doublet to the leptonic component of the messenger field. But in this approach the attractive feature of independence of initial conditions is lost – another consequence that we wish to avoid here.

B. BBN Consistency

Since the abundance of dark matter (in our case consisting of gravitinos) is $\Omega_{\tilde{G}}h^2 = 0.110 \pm 0.006$ [26], substituting the minimal reheating temperature $T_R^{(\rm min)}$ discussed above into (1) shows that the gravitino mass consistent with the dark matter abundance is at least $\mathcal{O}(1\,{\rm GeV})$ in the most optimistic case of the gaugino masses degenerate with $m_{\rm NLSP}$. With such gravitino masses the NLSP lifetime,

$$\tau_{\rm NLSP} = \left(5.9 \cdot 10^4\,{\rm sec}\right) \left(\frac{m_{3/2}}{1\,{\rm GeV}}\right)^2 \left(\frac{100\,{\rm GeV}}{m_{\rm NLSP}}\right)^5 \qquad (2)$$

for $m_{3/2}/m_{\rm NLSP} \ll 1$, easily exceeds the duration of the big bang nucleosynthesis. NLSP decays taking place during or after BBN, can alter its successful predictions if the relic abundance of the NLSP and/or the hadronic branching fraction in the NLSP decay is large enough [27–38]. Furthermore, if the NLSP is charged, it can bind with nuclei, which facilitates the production of ^{6}Li [39–41]. This introduces a tension between successful thermal leptogenesis, which requires $T_R > T_R^{(\rm min)}$, and gravitino Dark Matter. For a given MSSM spectrum and known $\Omega_{\rm NLSP}h^2$ this tension can be translated with (1) and (2) into a lower bound on $\tau_{\rm NLSP}$ and an upper bound on $m_{3/2}$.

The BBN bounds are weaker and more easily satisfied for shorter lifetimes, see also [42–45], and disappear

below 0.1 s. Therefore, there has been an effort to identify the NLSP candidates for which the BBN bounds are weaker than usual, hence allowing for relatively heavy gravitino DM and a high reheating temperature. Several solutions have been proposed, involving either a reduction of the NLSP relic abundance compared to the generic case, see *e.g.*, [46–48], or the suppressing of the energy released in the NLSP decay kinematically, thanks to extremely small mass splitting between the NLSP and the gravitino LSP [49].

The type of NLSP also plays an important role and changes the BBN bounds. One of the most studied is the stau: it naturally is the NLSP in minimal models of gauge mediation with a large messenger number and a high scale of supersymmetry breaking (the latter feature also predicts a heavy gravitino), and in its decay few energetic hadrons dangerous to BBN are produced. Nevertheless, the stau is charged and it is constrained by bound-state effects, so for a typical stau relic abundance, a reheating temperature larger than $\mathcal{O}(10^8\,\mathrm{GeV})$ is excluded, even with a compressed spectrum of stau and gaugino masses [8]. Stau relic density can also be suppressed thanks to a large left-right mixing in the stau sector. This effect has been studied in the context of the CMSSM and possible reheating temperatures as large as. $\sim 10^9\,\mathrm{GeV}$ for $\mu < 0$ [46] and $\mathcal{O}(10^8\,\mathrm{GeV})$ for $\mu > 0$ [50] were found. There is also a possibility that the stau annihilation cross section is enhanced by a Higgs pole [51]. All these solutions require a fine tuning among the soft supersymmetry breaking mass parameters.

Sneutrinos as the NLSP easily evade the BBN bounds even for a high reheating temperature suitable for thermal leptogenesis, as long as their masses do not exceed 200-300 GeV [52, 53]. Hovewer, arranging for a sneutrino NLSP requires a strong degeneracy between the soft supersymmetry breaking mass parameters for the superpartners of the left- and right-handed leptons (see [8] for gauge mediation) or non-universal Higgs masses (see [54–56] for gaugino and gravity mediation).

Therefore, our interest turns to a relatively unexplored option, that of thermal leptogenesis with a neutralino NLSP and a general spectrum of supersymmetric particles, as most recent studies on neutralino NLSP were done in the context of CMSSM with a gravitino LSP. In the next section we shall describe the challenges of this option, then do the quantitative work in sec. II to show that it can work under some circumstances, and then describe the LHC implications in sec. III.

C. Leptogenesis with Neutralino NLSP

At first sight, neutralinos as candidates for the NLSP appear much worse than sleptons or sneutrinos [34]. First, hadrons are often found in the decay channels of the neutralinos (roughly, the hadronic branching fraction B_h ranges from 3 to 50 percent for neutralino masses between 100 and 1000 GeV [47]). Secondly, the bino NLSP usually has a large relic abundance and it has been considered mostly in the context of models with universal gaugino masses, i.e. with M_r/g_r^2 independent of the gauge group index r at the scale of supersymmetry breaking[1]. With the gluino mass approximately 5 times larger than the bino mass at the electroweak scale, it is clear from eq. (1) that the resulting reheating temperature is smaller by an order of magnitude with respect to the case of little or no hierarchy between the gaugino masses. As will become evident in the figures of sec. II, the typical maximum reheating temperature for the bino NLSP with universal gaugino masses reaches only $10^5 - 10^6$ GeV, which is much too low for successful thermal leptogenesis needs.

Reconciling models of gauge mediated supersymmetry breaking with thermal leptogenesis requires either lowering the leptogenesis temperature or relaxing the BBN bounds. As discussed above, this can be achieved simply by reducing the relic density of the NLSP *e.g.* by means of coannihilations with more strongly interacting particles (which also evades strong cosmological bounds on the presence of metastable charged or strongly interacting particles). Reducing the NLSP relic density by coannihilations remains largely unexplored phenomenologically, expecially in this context, but has been explored for the case of bino-stau coannihilation in the CMSSM [31, 35, 36, 42–44, 50] or in more general models [47].

In the following, we would like to focus on the most promising case of neutralino/gluino mass degeneracy. We determine if the reheating temperatures allowed in such a scenario are consistent with thermal leptogenesis and what fine tunings may be necessary. This part of our discussion depends only on the assumption that gravitinos are the dark matter particles, and we assume arbitrary masses of the supersymmetric particles, without imposing constraints from specific theoretical models. Note that for bino and wino NLSP, the gaugino masses play a domininant role in the gravitino and NLSP abundances, and a degeneracy helps to reduce both. Therefore the degenerate spectrum can be considered the best case scenario.

II. MAXIMIZING THE REHEATING TEMPERATURE

Whether a given set of the parameters leading to gravitino LSP and a neutral NLSP is consistent with the BBN bounds depends mainly on 4 quantities: the NLSP

[1] At 1 loop, M_r/g_r^2 is a renormalization group invariant; for concretness, we impose the universality condition at the boundary scale 10^{15} GeV.

mass, its relic abundance, its hadronic branching fraction and its lifetime (which can be traded for $m_{3/2}$ with the use of (2)). Refs. [37, 38] find the excluded regions on the $(\tau_{\rm NLSP}, \Omega_{\rm NLSP}h^2)$ plane for different values of the hadronic branching fraction and two values of the NLSP masses, 100 and 1000 GeV. Up to a moderate shift in the allowed $\Omega_{\rm NLSP}h^2$, the excluded regions are very similar for both these masses. In order to apply the BBN bounds for a general set of parameters, we interpolate (linearly on a logarithmic scale) between the results of [37, 38], constructing the maximal allowed NLSP abundance, $\Omega^{\rm max}_{\rm NLSP}h^2(m_{\rm NLSP}, \tau_{\rm NLSP}, B_h)$. Using this function, for a given MSSM spectrum, we can calculate $\Omega_{\rm NLSP}h^2$, find the maximal $m_{3/2}$ for which $\Omega_{\rm NLSP}h^2 < \Omega^{\rm max}_{\rm NLSP}h^2$ and, from (1), find the maximal allowed reheating temperature.

In general, $\Omega^{\rm max}_{\rm NLSP}h^2$ decreases with growing B_h, but it is a non-monotonic function of $\tau_{\rm NLSP}$: it consists of 4 convex parts, reflecting the bounds for the abundance of ^{4}He, D, ^{6}Li and ^{3}He. Since for increasing NLSP mass the predicted $\Omega_{\rm NLSP}h^2$ and B_h increase, at certain values of $m_{\rm NLSP}$, we may find the BBN-allowed regions (around local maxima of $\Omega_{\rm NLSP}h^2$ as a function of $\tau_{\rm NLSP}$) close. This makes the bounds for $m_{3/2}$ and T_R discontinuous functions of $m_{\rm NLSP}$.

In the case of no coannihilations, we calculate the NLSP relic density with the computer code `micrOmegas` [57, 58]. In the case with neutralino/gluino degeneracy we include the coannihilations (taking into account nonperturbative contributions) using the prescription described in detail in Appendix A. For hadronic branching fractions for bino, wino and higgsino NLSP we use the results obtained in [47], while we take it equal to 1 in the gluino NLSP case.

A. Bino NLSP

Our results for bino NLSP are shown on Figures 1, 2 and 3. The maximal allowed $m_{3/2}$, corresponding in practice to the largest reheating temperature, can be directly obtained from the BBN bounds. Figure 1 shows the predictions for $\Omega_{\rm NLSP}h^2$ for three cases: without degeneracy with gluino, with 10% and 1% degeneracy, together with the BBN bounds for three different values of the gravitino mass, $m_{3/2} = 0.1, 1, 10\,{\rm GeV}$ and two values of $B_h = 0.01, 1$. In the case of non-degeneracy, it is necessary to know the remaining susy spectrum for the purposes of computing the bino relic abundance. For that, we have chosen the spectrum of minimal gauge mediation with one $\mathbf{5} + \bar{\mathbf{5}}$ messenger pair and the messenger mass of $10^{15}\,{\rm GeV}$. For such a spectrum the main contributions to the bino pair annihilations come from t-channel slepton exchanges and the bino-to-slepton mass ratio is approximately 0.4. Since the bino annihilation cross-section is proportional to $1/m^4_{\tilde\ell}$, by increasing this

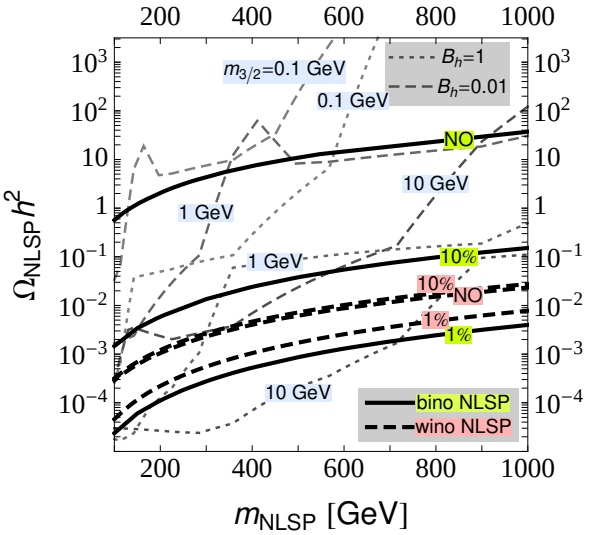

FIG. 1: Gray dashed lines show the BBN bounds on $(m_{\tilde B}, \Omega_{\rm NLSP}h^2)$ plane for three different values of the gravitino mass, $m_{3/2} = 0.1, 1, 10\,{\rm GeV}$ and two values of $B_h = 0.01, 1$ Also shown are predictions for $\Omega_{\rm NLSP}h^2$ for the non-degenerate NLSP case (labeled *NO*) and with NLSP/gluino degeneracy of 10% and 1%; thick black solid (dashed) lines correspond to the bino (wino) NLSP.

ratio (e.g. increasing the numbers of messengers in minimal gauge mediation), one can suppress the resulting $\Omega_{\rm NLSP}h^2$. However, even with 1% bino/slepton mass degeneracy, $\Omega_{\rm NLSP}h^2$ is smaller only by a factor of ~ 20 compared to our reference case, so it is still larger than what we obtain with 10% bino/gluino mass degeneracy.

Figure 2 translates these results into the largest allowed $m_{3/2}$ for each of the three cases and Figure 3 shows the largest allowed reheating temperature for each case. Since the reheating temperature depends on the pattern of gaugino masses, we assume universal masses for the case without degeneracy and a pattern $M_1 : M_2 : M_3 \approx 1 : 2 : 1$ for the degenerate cases.

We see that with 1% bino-gluino mass degeneracy, we are able to reach a reheating temperature as high as a few $10^9\,{\rm GeV}$ with $m_{\tilde B} < 300\,{\rm GeV}$. Even with only 10% bino-gluino mass degeneracy, we are able to reach $T_R \gtrsim 0.7 \cdot 10^8\,{\rm GeV}$ for bino masses all the way up to 1 TeV.

B. Wino NLSP

Our results for wino NLSP are also shown on Figures 1, 2 and 3 in the same way as for the bino NLSP case. The only difference is instead of the universal gaugino mass pattern, which always gives the bino as the lightest gaugino, we use the spectrum arising in models with anomaly mediated supersymmetry breaking (AMSB) [59, 60]. This serves as a good illustration of a

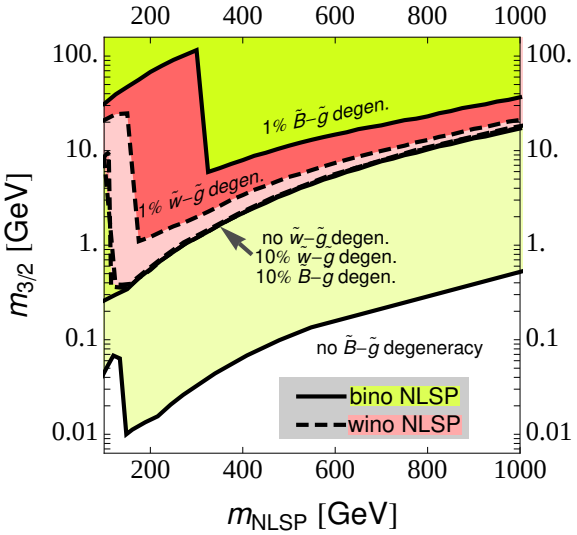

FIG. 2: BBN bounds on $(m_{\tilde{B}}, m_{3/2})$ plane for the non-degenerate NLSP case (labeled *no* $\tilde{B}-\tilde{g}$ *(*$\tilde{w}-\tilde{g}$*) degeneracy*) and with NLSP/gluino degeneracy of 10% and 1%; thick black solid (dashed) lines correspond to the bino (wino) NLSP

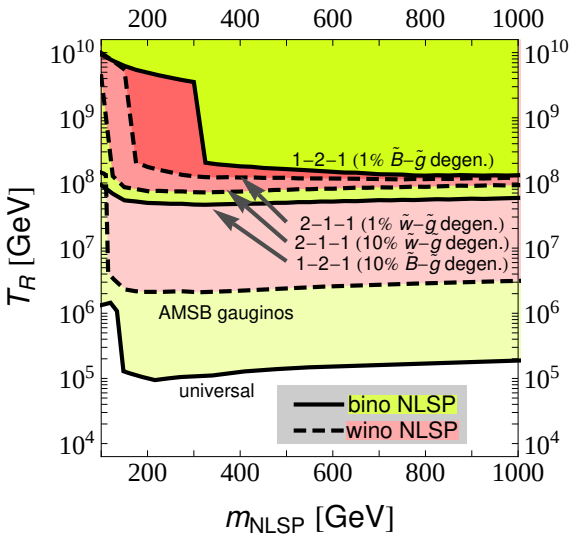

FIG. 3: BBN bounds on $(m_{\tilde{B}}, T_R)$ plane. Solid lines correspond to the bino NLSP case with universal gaugino masses and to bino/gluino degeneracy of 10% and 1% with $M_1 : M_2 : M_3 \approx 1 : 2 : 1$ (labeled 1-2-1). Dashed lines correspond to the wino NLSP case with AMSB gaugino mass spectrum and to wino/gluino degeneracy of 10% and 1% with $M_1 : M_2 : M_3 \approx 2 : 1 : 1$ (labeled 2-1-1).

theory approach giving the wino as the lightest gaugino.

Models with nondegenerate wino NLSP allow for a reheating temperature from a few 10^6 GeV for the AMSB gaugino spectrum, with $m_{\tilde{g}} \sim 10\, m_{\tilde{w}}$, to a few 10^7 GeV for milder mass hierarchies (given by the 10% $\tilde{w}-\tilde{g}$ degeneracy line with almost the same $\Omega_{\rm NLSP}h^2$ as the nondegenerate case). Although such T_R is larger than in the models with the generic bino NLSP, a degeneracy with a gluino helps less or does not even help at all in reducing $\Omega_{\rm NLSP}h^2$. It can be seen from eq. (5) in Appendix A that, in the limit of a very strong degeneracy, $(m_{\tilde{g}}/m_{\rm NLSP} - 1) \to 0$, and a dominant gluino annihilation cross section, the resulting effective annihilation cross section is proportional to $(16+g)^{-2}$, where $g = 2\,(6)$ is the number of the NLSP degrees of freedom for bino (wino) NLSP. Therefore we expect the effective cross-section for the wino to be smaller than for the bino and the wino abundance to be larger by $\sim (11/9)^2 \approx 1.5$. Considering as well that the wino hadronic branching ratio is a factor $\tan^{-2}\theta_W \sim 3.3$ larger than for the bino, the stronger bound is explained. We see that a reheating temperature of a few 10^9 GeV is also possible in the wino NLSP case with a 1% wino-gluino mass degeneracy, but due to the above effects such large reheating temperatures are possible only in the low mass region, for $m_{\tilde{w}} < 200$ GeV. Note that a light wino window, with masses around 100 GeV, is present also for the pure wino case, without coannihilations with the gluinos [47].

We also note that a 10% wino/gluino degeneracy actually increases the NLSP relic density despite a larger annihilation cross section for gluinos, as it can be seen in Figure 9 as a little 'bump' in the predictions for $\Omega_{\rm NLSP}h^2$ in the wino NLSP case. This happens due to the presence of the 'weights' γ_i^2 in (5), obeying $\gamma_0 + \gamma_{\tilde{g}} = 1$, and the fact that the real coannihilation cross-section involving a wino and a gluino in the initial state is negligible for larger squark masses. In this case, as discussed in the appendix A, the effective cross-section reaches a minimum when the ratio of the gluino over wino weights is equal to the ratio of the wino over gluino cross-sections. The increase in the abundance is at most $1 + \sigma_0/\sigma_{\tilde{g}}$, so it is negligible for the bino case, but visibile for the wino.

C. Higgsino NLSP

The case of higgsino NLSP in models of gauge mediation is more involved. Although arranging for cancellations between various contributions to the soft sypersymmetry breaking Higgs mass parameter $m_{H_2}^2$, and hence μ parameter, is most welcome phenomenologically, it requires some fine tuning in the boundary conditions. Furthermore, for light neutralinos, the hadronic branching fraction is quite sensitive to the gaugino admixture and, *e.g.*, 5% bino content can lower B_h even by an order of magnitude [47]. Moreover a non-vanishing gaugino fraction opens up also the channel of resonant annihilation via the pseudoscalar Higgs so that the higgsino number density can vary strongly around $2m_{\tilde{h}} \sim m_A$. For these reasons, we only indicate here the predictions for the higgsino NLSP in the conservative case of no resonant annihilation. With the gauginos twice heavier than the higgsino, we obtain the maximal reheating temperature

$(2-3)\times 10^7$ GeV for higgsino masses between 100 and 1000 GeV and 5% bino admixture. Larger reheating temperatures are surely possible if the annihilation proceeds on the resonance, at the cost of a fine-tuning between the neutralino and Higgs masses [47].

For the case of a higgsino NLSP, coannihilation with the gluinos is perhaps less natural since one could expect all the gauginos to be much heavier than the higgsinos. Also the equilibrium between higgsinos and gluino mainly proceeds through small Yukawa couplings and is somewhat less effective than for gauginos. Finally, one needs to know the full spectrum of the higgsinos to account for the effective number of the degrees of freedom participating in coannihilations. This can vary from 8, if the mass splittings among the higgsinos are not larger than with the gluino, to 2, if the mass gap between the lightest higgsino and the gluino is much smaller than the mass splittings among the higgsinos. The former case requires decoupling of heavy binos and winos: a situation with an extreme fine-tuning of the input parameters at the high scale of supersymmetry breaking and, as we have already seen in the wino NLSP case, a large number of coannihilating states leads to larger $\Omega_{\rm NLSP}h^2$; hence, the latter case appears more plausible.

We explored nevertheless the possibility of higgsino/gluino coannihilations within models of general gauge mediation with the messenger scale 10^{15} GeV. We found an intermediate result between bino and wino neutralino: the annihilation cross-section lies between those for bino and wino NLSP, and in the limit of strong NLSP/gluino degeneracy one higgsino participates in coannihilations much more efficiently than the others. For a 300 GeV higgsino, we obtain the relic density of a few 10^{-4}, while at the Higgs resonance it goes down to a few 10^{-5}.

D. Gluino NLSP

Although gluino NLSP has a small relic density, with $\Omega_{\rm NLSP}h^2$ ranging from $6\cdot 10^{-5}$ to $2\cdot 10^{-3}$ for gluino masses from 200 to 1000 GeV, successful primordial nucleosynthesis places very stringent limits on the presence of long-lived strongly interacting relic particles after the BBN [61]. If the NLSP is coloured, its lifetime should not exceed 300 sec and this is the origin of the constraint $T_R < 3-7\cdot 10^7$ GeV for $m_{\tilde g}$ ranging from 200 to 1000 GeV and the bino and the wino twice as heavy as the gluino. We also note here that the gluino NLSP relic density is smaller than the relic density of a stop with the same mass [62], hence the maximal allowed reheating temperature in the stop NLSP case is lower than for the gluino NLSP.

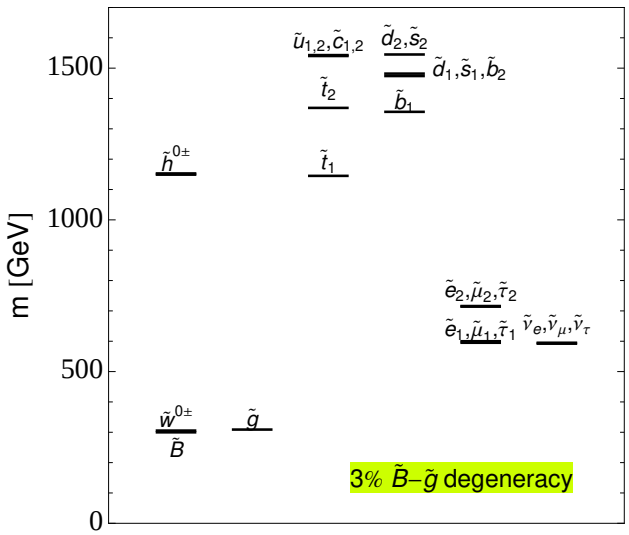

FIG. 4: Mass spectra of sparticles in the example discussed in the text. The lowest neutralino line corresponds to $m_{N_1} = 299.8$ GeV, $m_{N_2} = 305.6$ GeV and $m_{C_1} = 305.6$ GeV, while $m_{\tilde g} = 308.9$ GeV. The Higgsino mass parameter is $m_{\tilde H} = 1153$ GeV and is irrelevant to the ensuing discussion.

III. LHC DISCUSSION

Taking into consideration the requirements of CP asymmetries, BBN, and gravitino dark matter, we have concluded that an interesting approach to viable leptogenesis leads to nearly degenerate gauginos and a spectrum of scalar superpartners somewhat higher in mass. In particular, the gluino mass needs to be rather close in value to the NLSP mass such that coannihilation effects can sufficiently reduce the number density of the NLSP so as to not disrupt BBN when the NLSPs decay. This generic feature of the spectrum has important consequences for LHC discovery of supersymmetry.

A. Gluino pair production

If the gauginos are much lighter than the scalars, then the largest supersymmetry production cross section at the LHC is $\tilde g\tilde g$. In the limit of a nearly exact degeneracy of the neutralino NLSP and gluino masses, there are no visible particles to trigger on from the production and decay of gauginos, since the final state is just an invisible neutralino and a very soft gluon or $q\bar q$ pair. For extreme degeneracy below a percent or two, the gluino decay is strongly suppressed and a displaced vertex at ≥ 1 mm distances is possible, but again generally with no visible particle to trigger on, only one or two very soft jets.

For illustration of the issues of detectability of supersymmetric particles at the LHC, we shall take a closer look at the model with mass spectrum shown in Fig-

channel	branching fraction
$\tilde{g} \to N_1 g$	0.59
$\tilde{g} \to N_1 q\bar{q}$	0.35
$\tilde{g} \to N_2 g$	0.03
$\tilde{g} \to N_2 q\bar{q}$	0.02
$N_2 \to N_1 \nu\bar{\nu}$	0.41
$N_2 \to N_1 \gamma$	0.31
$N_2 \to N_1 \ell^+\ell^-$	0.08

TABLE I: Branching fractions relevant for collider analysis.

ure 4. This model can be realized within the framework of general gauge mediation with the messenger scale of 10^{15} GeV and $\tan\beta = 10$. Bino/gluino degeneracy is 3% and the resulting maximal reheating temperature attainable in this model is $3 \cdot 10^8$ GeV. From the branching fractions in table I we see that over 1/3 of the $\tilde{g}\tilde{g}$ events will be in the most advantageous channel $\tilde{g}\tilde{g} \to gN_1gN_1$, or in other words, two jets plus missing energy.

For our example model point, the gluino mass is 309 GeV and the leading order total cross-section at $\sqrt{s} =$ 14 TeV LHC is $\sigma(\tilde{g}\tilde{g}) \simeq 255 \pm 5$ pb. Thus, in a few fb^{-1} of data we expect quite a large number of events from $\tilde{g}\tilde{g}$. However, it will be difficult to trigger on these events and discern them above a large background. To see this, we note that in the rest frame of the gluino the energy of the gluon is fixed to be $E_g = (m_{\tilde{g}}^2 - m_{N_1}^2)/(2m_{\tilde{g}}) = 9.0$ GeV.

We have conducted a MadGraph [63] Monte Carlo simulation of the production of gluino pairs followed by decay into gluon plus neutralino. The results are given in Figure 5, where we have plotted the p_T values of each jet at the parton level. Each event is a point in the (p_{T_1}, p_{T_2}) plane, where p_{T_1} is the higher p_T of the two jets. The gluon energy in the lab frame may increase or decrease depending on its relative decay direction to the boost direction. For this reason, the highest p_T jet can be rather large – in this simulation of 1000 events, the highest p_T obtained was nearly 60 GeV.

Unfortunately, the visible energy and missing energy is not enough to trigger the events for saving at the LHC. There is too much background to open the trigger to events of this kinematic topology without significant prescaling that loses the signal. For example, for $\sqrt{s} = 7$ TeV collisions, where the LHC is currently running, there are several triggers that are of potential relevance to gluino gluino production followed by decays to soft things [64]; however, each fails to capture a significant number of signal events. There is the "single jet" trigger requiring $p_T \gtrsim 110$ GeV, the "dijet trigger" which requires the average $p_T > 70$ GeV, the "sum p_T" trigger which requires $p_T^{\rm sum}(\text{jets}) > 200$ GeV, and the non-prescaled "missing E_T" trigger requiring MET > 60 GeV. These are only for the 7 TeV collider, and each of these numbers will be approximately doubled for the 14 TeV collider. Thus, none of these triggers will efficiently record these events, and we seek a better path to discovery.

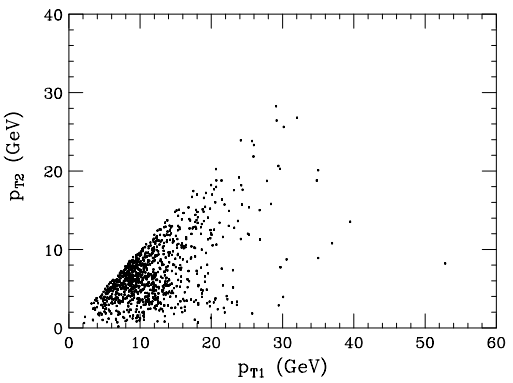

FIG. 5: Scatter plot of p_T values for the two gluons in $\tilde{g}\tilde{g} \to gN_1gN_1$ for 1000 events with $m_{\tilde{g}} = 308$ GeV and $m_{N_1} = 300$ GeV. This simulation is for a pp collider with $\sqrt{s} = 14$ TeV center of mass energy.

When gaugino degeneracy is present, we have seen that the final states in the process are too soft to trigger on. Therefore, we need another process that can generate much higher p_T jets or leptons. We remark that there is also the prospect of detecting gluino pair production via tagging from an initial state radiation (ISR) jet. This is a technique that has been advocated for many new physics scenarios that have no substantial visible energy from the final state [65]. ISR jets tend to be soft, and backgrounds are determined to large degree by how well the detector is understood and how well fake rates and jet energy measurements can be controlled. We do not pursue this approach here, but merely remark that it could be a useful signal for discovery, or even confirming a model if discovery is made through another channel. It would be especially important in the case of very high degeneracy such that the gluino decay has a displaced vertex, as discussed earlier in the section.

B. Squark-gluino monojet signature

We wish to determine if there might yet be another signature of value. Upon inspection of the spectrum it is evident that squarks are too heavy to pair produce efficiently, and certainly the same goes for the more weakly coupled sleptons. However, the squarks are often not too heavy for the promising signature of a single squark being produced in association with a (much lighter) gluino.

An important contributing factor to the viability of

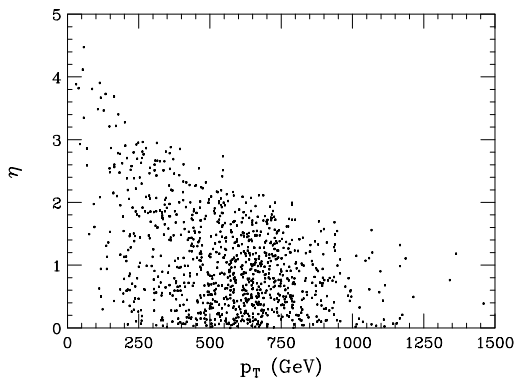

FIG. 6: Scatter plot of 1000 events at $\sqrt{s} = 14\,\text{TeV}$ pp collider from $\tilde{q}\tilde{g} \to q\tilde{g}\tilde{g}$, where $m_{\tilde{g}} = 300\,\text{GeV}$ and $m_{\tilde{q}} = 1.5\,\text{TeV}$. The meaning of $\tilde{q}$ is all first and second generation squarks: $\tilde{u}_L$, $\tilde{u}_R$, $\tilde{d}_L$, $\tilde{d}_R$, $\tilde{s}_L$, $\tilde{s}_R$, $\tilde{c}_L$, $\tilde{c}_R$. Each event is characterized by the absolute value of the pseudorapidity η of the quark jet from $\tilde{q} \to q\tilde{g}$ decays, and the p_T of that jet. Given that the gluino is nearly degenerate with all other gauginos including the NLSP, it acts like a source of missing energy. Thus, the p_T of the quark jet is approximately the missing energy of the event also.

this signature is the high parton luminosities for gq initial states that produce $\tilde{g}\tilde{q}$ at tree-level. Furthermore, the kinematics of these events are favorable where the large mass difference between the squark and gluino generates a large p_T jet from $\tilde{q} \to \tilde{g}q$ decays. There is a also a large amount of missing energy recoiling against this jet. The signature is that of monojet plus missing energy. This has been studied recently within the context of the Tevatron for a wide class of models [66], as well as studies dedicated to the LHC, as we shall discuss below. Gluino pair production with ISR jet discussed in the previous section can also contribute to this signature, although the jet p_T is typically much softer. We shall ignore that additional small contribution to the high p_T signal defined in the following analysis.

The model that we simulate is a slightly simplified version of our spectrum that we considered above. We consider here $m_{\tilde{g}} = 300\,\text{GeV}$ and take the light squark masses to be 1.5 TeV in order to illustrate the signature with a reasonable spectrum. Generically, and certainly in this case, over 90% of light squark decays are into $\tilde{q} \to q\tilde{g}$, so single jet plus missing energy (i.e., soft-invisible decays of gluinos) becomes the most important signature to consider. The total leading order production cross-section at the 14 TeV pp LHC collider is 3.4 pb. Although this is nearly two orders of magnitude below the $\tilde{g}\tilde{g}$ cross-section, the picobarn rate is high enough to record many thousands of events in the course of a few inverse femtobarns of integrated luminosity. Thus, it is a promising signature. In Figure 6 1000 events are simulated, where we give the pseudorapidity (η) and the p_T values for each simulated event. To reduce backgrounds and increase reliability of the analysis, it is often required that the jet be central ($|\eta| < 2$) and have large p_T ($p_T > 200\,\text{GeV}$). Those two requirements still leave the vast majority of events available for analysis.

Figures 7 and 8 plot the total squark plus gluino production cross-section at a 7 TeV and 14 TeV center of mass energy pp collider as a function of the squark mass (first two generations) for various values of the gluino mass. When the squark mass is much greater than the gluino mass, the resulting jet p_T from squark decays to gluino plus quark are very high, and we get a strong single jet plus missing energy signature with very high trigger efficiency.

The question of what the background is for the single jet plus missing energy is notoriously subtle. Our purposes here are to describe the basic features of the background, and give an estimate of expectations. Only a full detector simulation after careful engagement with the LHC data can ultimately determine what precise sensitivity levels can be reached.

Nevertheless, we can compare our signal to the background after cuts advocated in table 2 of [67]. First, the majority of our signal will be one jet plus missing energy. Multiple jets will arise from higher order corrections, which increases the signal; however, we do not include these, thereby losing out on small additional signal, but also not being affected adversely by the "Number of jets < 3" cut implemented by [67]. Nevertheless, we know that that cut is very important in reducing $t\bar{t}$ and QCD backgrounds, and we can assume with overall impunity to the signal that it has been applied to the background. We can also apply $E_T^{\text{miss}} > 400\,\text{GeV}$, which, given that we are working to leading order, automatically also implies the simultaneously required $p_T(jet) > 350\,\text{GeV}$. It is automatic because at our leading order computation $p_T(jet) = E_T^{\text{miss}}$ to a good approximation. We can also require that the pseudo-rapidity of our jet is less than 1.7 as [67] requires. The remaining two azimuthal angle cuts in table 2 of [67] have no consequence to us because they are automatically satisfied in our approximation. Furthermore, they have little effect on the larger backgrounds anyway.

The combination of $E_T^{\text{miss}} > 400\,\text{GeV}$ and $\eta_{jet} < 1.7$ tends to reduce our signal by only $\sim 30\%$ which is within the uncertainty of QCD corrections and other uncertainties of the analysis. For the background, if we combine all these cuts we get approximately less than 50 events per $100\,\text{pb}^{-1}$ of data. In other words, the background is about 0.5 pb. This estimate is also consistent with the results of refs. [68, 69]. Furthermore, these backgrounds can be measured well since at high missing E_T they are dominated by $Z(\nu\bar{\nu}) + j$ which can be normalized to the $Z(l^+l^-) + j$ rate. Thus, assuming accurate computations

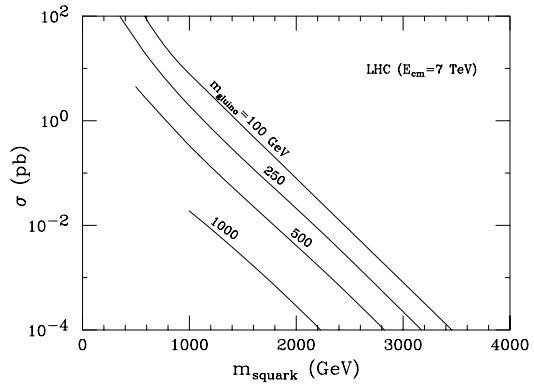

FIG. 7: Squark gluino production cross-section at $\sqrt{s} = 7\,\text{TeV}$ pp collider as a function of squark mass for various values of the gluino mass. The squark masses refer to first two generation squarks.

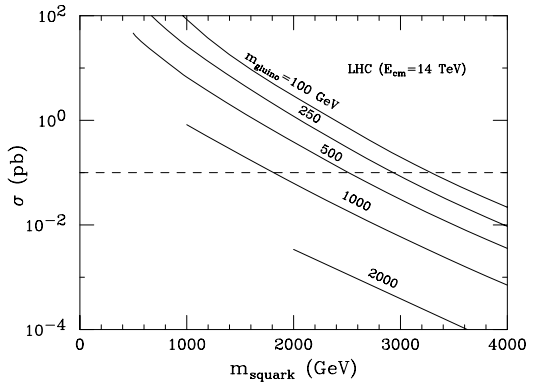

FIG. 8: Squark gluino production cross-section at $\sqrt{s} = 14\,\text{TeV}$ pp collider as a function of squark mass for various values of the gluino mass. The squark masses refer to first two generation squarks. The dashed line of $\sigma = 0.1\,\text{pb}$ is the estimated lower limit of the cross-section that the LHC would be sensitive to when seeking a BSM contribution after more than $1\,\text{fb}^{-1}$ of data is accumulated.

and measurements can be done for the background, and uncertainties can dip below 20%, we estimate reaching sensitivities down to approximately the 0.1 pb level for the signal. In $1\,\text{fb}^{-1}$ of data, for example, we would have about 100 signal events at that cross-section, and results would be very near threshold for detectability. Thus, we can tentatively conclude that the 0.1 fb cross-section line is approximately the threshold for discovery of BSM singlet jet plus missing energy signature at 14 TeV LHC. From that determination, everything above the dashed 1 pb line in Figure 8 may be detectable at the LHC with over $1\,\text{fb}^{-1}$ of data. Generically this leads to discovery sensitivity of gluinos less than $\sim$ TeV with squarks above even a few TeV.

C. Tevatron Remarks

The parameter space we have been considering is where the gauginos, including gluino, are nearly degenerate. We should remark on what bounds there might be at the Tevatron for this scenario, if any. The limits on the gluino mass from CDF and D0 experiments are usually quoted to be above $\sim 300\,\text{GeV}$ [70]; however, those limits assume that the gluino decays into an LSP of much lower mass such that the visible energy in the event is very high and can be triggered on. That is not the case in our model. The true capability of a limit should be much lower.

When the gluino mass is degenerate with the LSP to within 10 GeV, the Tevatron has the potential to exclude its existence up to 160 GeV when the lumonisity exceeds $2\,\text{fb}^{-1}$ [71]. The signal is gluino pair production in association with a jet, leading to a monojet plus missing energy signature. Signal to background requirements are unlikely to allow improvement beyond 160 GeV even with greater luminosity [71]. It has been suggested [72] that the photon plus missing energy signature could be more probing than the monojet plus missing energy signature when luminosity exceeds $1\,\text{fb}^{-1}$. Although the signal is lower, the signal to background is higher for any given gluino mass, and with sufficient luminosity the higher signal to background signature always wins in sensitivity. The probing sensitivity for gluinos nearly degenerate with LSP in the photon plus missing energy channel with greater than $1\,\text{fb}^{-1}$ has been estimated to be 175 GeV [72]. Further discrimination from background may be possible in some cases if gluino decays frequently produce leptons, albeit very soft ones, through intermediate chargino or neutralino decays to the LSP. We are not aware of any Tevatron experimental paper that has reported an analysis for these scenarios, so the numbers above are suggestive of what could be done, and not what has been achieved yet.

IV. SUMMARY & CONCLUSIONS

In the case of a gravitino LSP and DM, we have explored the parameter space of neutralino NLSP with a nearly degenerate gluino and we found that the BBN constraints are strongly relaxed in the bino case, so that a reheating temperature sufficiently high for thermal lep-

togenesis and the right gravitino abundance are obtained just with a mass degeneracy of the order of a few percent between bino and gluino. So in general a compressed gaugino spectrum helps in reconciling leptogenesis with gravitino DM and neutralino NLSP. On the other hand, for the wino and higgsino cases, the coannihilation with gluinos does not improve much the situation: for the wino case, it extends a bit the light wino window already found in [47] for a pure wino, while for the higgsino it does not beat the abundance suppression that can be obtained through the resonant annihilation. We found also that these degenerate gaugino scenarios can be embedded in general gauge mediation with a moderate tuning of the parameters, but since our results depend mostly only on the gaugino masses they are not restricted to these specific case and can be extended to any supersymmetry breaking scenario that allows for degenerate gaugino masses.

In all these cases though, the gluinos are not only nearly degenerate with the NLSP, but also quite light ≤ 300 GeV and are therefore copiously produced at the LHC. The fact that gravitino DM and thermal leptogenesis together give an upper bound on the gluino mass around the TeV scale was well-known [73], but in our case in order to suppress the NLSP number density we need also a light NLSP and gluino. Unfortunately, since the degeneracy between them is small, even if the production cross-section is large, the main signal of a highly energetic track is missing and it is not so simple to disentangle the scenario from the QCD background. We suggested a couple of final states and discuss if they could pass most of the LHC trigger cuts and some possible strategies for detection. The most promising channel is the gluino squark associated production, that gives a highly energetic jet in the final state and could be accessible even with $1\,\mathrm{fb}^{-1}$ of data during the early phase of running of the LHC.

Acknowledgments: We thank A. De Roeck, H. Flaecher, M. Nojiri for useful discussions.

SP thanks the Institute for Advanced Studies at TUM, Munich, for its support and hospitality. KT acknowledges the hospitality of the Theory Division at CERN and the MCTP.

LC acknowledges the support of the Deutsche Forschungsgemeinschaft under the Collaborative Research Centre 676. MO and SP acknowledge partial support by the European Research and Training Network (RTN) grant 'Unification in the LHC era' (PITN-GA-2009-237920) and by the MNiSZW scientific research grant N N202 103838 (2010 - 2012). KT is partially supported by the Foundation for Polish Science through its programme Homing.

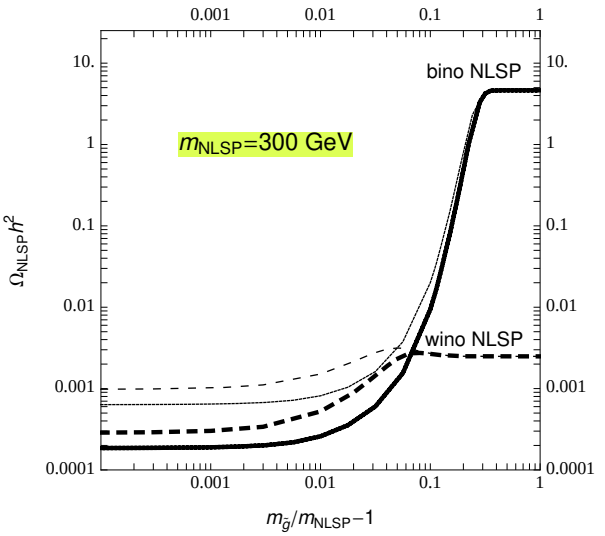

FIG. 9: NLSP relic density calculated in the presence of gluino coannihilations as a function of the degeneracy parameter $m_{\tilde{g}}/m_{\mathrm{NLSP}} - 1$ for $m_{\mathrm{NLSP}} = 300\,\mathrm{GeV}$. Solid (dashed) lines correspond to bino (wino) NLSP. Thick (thin) lines show the results with (without) nonperturbative contributions.

Appendix A: gluino coannihilations with Sommerfeld enhancement

Here we discuss how to include nonperturbative effects in the gluino annihilation, often referred to as Sommerfeld enhancement. Our calculation closely follows [74, 75].

With the NLSP of mass m, the freeze-out temperature is given by:

$$x_F = \ln\left[c(c+2)\sqrt{\frac{45}{8}}\frac{g_{\mathrm{eff}}}{2\pi^3}\frac{1}{\sqrt{g_* x_F}} m M_P \langle\sigma v\rangle\right], \qquad (3)$$

where $x = m/T$, c is the coefficient in the relation $Y = (1+c)Y^{\mathrm{eq}}$ (which we set to $1/2$), M_P is the Planck mass (not reduced), g_{eff} is the effective number of the degrees of freedom decoupling at freeze-out and $\langle\sigma v\rangle$ is the average containing the annihilation cross-section σ. The average is:

$$\langle\sigma v\rangle = \frac{1}{8m^4 T K_2^2\left(\frac{m}{T}\right)}\int_{4m^2}^{\infty}\sigma\, s^{3/2}\beta^2 K_1\left(\frac{\sqrt{s}}{T}\right)\mathrm{d}s \qquad (4)$$

with $\beta = \sqrt{1-4m^2/s}$.

We assume that the annihilation cross-section is the sum of the NLSP annihilation cross-section and the gluino coannihilation cross section:

$$\sigma = \gamma_0^2\sigma_0 + \gamma_{\tilde{g}}^2\sigma_{\tilde{g}\tilde{g}}\,, \qquad (5)$$

where $\gamma_0 = g_0/g_{\mathrm{eff}}$, $\gamma_{\tilde{g}} = 1-\gamma_0$,

$$g_{\mathrm{eff}} = g_0 + 16(1+\delta)^{3/2}e^{-\delta x}\,, \qquad (6)$$

$\delta = m_{\tilde{g}}/m_{\rm NLSP} - 1$ and g_0 is the number of the degrees of freedom of the NLSP and equals 2 (6) for bino (wino) NLSP. This approximation is justified in the limit of heavy squarks, necessary to satisfy the Higgs mass bound with light gluinos. In this case in fact the coannihilation channel $\tilde{\chi} + \tilde{g} \to q\bar{q}$ is strongly suppressed by the large squark masses and can be neglected. Note on the other hand that the processes in which a NLSP scatters inelastically off a SM particle to become a gluino are efficient down to the freeze-out temperature, as the suppression of the cross-section due to heavy squarks is compensated by a large abundance of the light SM states.

The neutralino annihilation cross-section includes many channels. For the gaugino neutralino case, an important annihilation channel at low neutralino masses is the one into leptons via intermediate sleptons, which are in our case much lighter than the squarks. This annihilation rate is given by

$$\sigma(\tilde{\chi}\tilde{\chi} \to \ell\bar{\ell}) = \frac{3\alpha|A_{L/R}|^2}{64\pi\cos^2\theta_W \beta_{\tilde{\chi}}^2 s}\left[\beta_{\tilde{\chi}} + \frac{4\beta_{\tilde{\chi}}\Delta^2}{(1+2\Delta)^2 - \beta_{\tilde{\chi}}^2} + \ln\left(\frac{1+2\Delta-\beta_{\tilde{\chi}}}{1+2\Delta+\beta_{\tilde{\chi}}}\right)\left(2\Delta + \frac{1-\beta_{\tilde{\chi}}^2}{2(1+2\Delta)}\right)\right], \quad (7)$$

where $\Delta = (m_{\tilde{\ell}}^2 - m_{\tilde{\chi}}^2)/s$ and

$$A_L = N_{j1} \pm N_{j2}\cot\theta_W \quad \text{for } \ell_L^-/\nu_{L\ell} \quad (8)$$

$$A_R = -2N_{j1}\,. \quad (9)$$

For larger masses and especially for the wino case, also the channel into W^+W^- becomes important and for the mixed case the resonant annihilation through the Higgs s-channel. In general in the case of wino neutralino also the coannihilation with the other charged winos is important and the cross-section is not very much smaller than the gluino annihilation cross-section. Since we consider spectra for which the sfermions are generally heavier than the superpartner fermions, we use an approximation $\sigma_0 \sim \beta/s$ ($\sigma_0 \sim 1/s\beta$) for bino (wino) NLSP, for which the p-wave (s-wave) annihilation dominates; the numerical coefficient is chosen so that it gives a correct relic density in the absence of coannihilations. In the case of the wino NLSP, one needs, in principle, to consider coannihilations between the wino states, but these states are typically extremely degenerate in mass, so σ_0 should be considered an effective cross section with a common γ_0 factor for all wino states in (5).

The gluino annihilation cross-section reads $\sigma_{\tilde{g}\tilde{g}} = \sigma(\tilde{g}\tilde{g} \to gg) + \sum_q \sigma(\tilde{g}\tilde{g} \to q\bar{q})$, where leading contributions, mediated by the gluons, are:

$$\sigma(\tilde{g}\tilde{g} \to gg) = \frac{3\pi\alpha_s^2}{16\beta_{\tilde{g}}^2 s}\left[\ln\left(\frac{1+\beta_{\tilde{g}}}{1-\beta_{\tilde{g}}}\right)(21 - 6\beta_{\tilde{g}}^2 - 3\beta_{\tilde{g}}^4) - 33\beta_{\tilde{g}} + 17\beta_{\tilde{g}}^3\right] \quad (10)$$

$$\sigma(\tilde{g}\tilde{g} \to q\bar{q}) = \frac{\pi\alpha_s^2\beta_q}{16\beta_{\tilde{g}} s}(3-\beta_{\tilde{g}}^2)(3-\beta_q^2)\,, \quad (11)$$

with $\beta_a = \sqrt{1-4m_a^2/s}$. The contribution of the cross-section with intermediate squarks is negligible in this case.

We see from the expression of the effective cross-section eq. (5), that the effective numbers of degrees of freedom γ change strongly with the temperature: defining as a variable the ratio $z = \gamma_{\tilde{g}}/\gamma_0$ it is easy to see that

$$\sigma = \sigma_0 \frac{1 + z^2\sigma_{\tilde{g}\tilde{g}}/\sigma_0}{(1+z)^2}\,, \quad (12)$$

and one can show that the fraction on the r.h.s. has minimum as a function of z at $\bar{z} = \sigma_0/\sigma_{\tilde{g}\tilde{g}}$ and that the minimal value is given as

$$\sigma = \sigma_0 \frac{1}{1+\bar{z}} = \sigma_0 \frac{\sigma_{\tilde{g}\tilde{g}}}{\sigma_{\tilde{g}\tilde{g}} + \sigma_0}\,. \quad (13)$$

So it is easy to see that this reduction of the cross-section is usually negligible for the case of bino neutralino, since $\sigma_0 \ll \sigma_{\tilde{g}\tilde{g}}$, but not for the wino.

The Sommerfeld enhancement is accounted for by multiplying each of the cross-sections (10) and (11) by the factor

$$E_i = \frac{\frac{C_i\pi\alpha_s}{\beta_{\tilde{g}}}}{1 - \exp\left(-\frac{C_i\pi\alpha_s}{\beta_{\tilde{g}}}\right)}\,, \quad (14)$$

where $C_i = 3/2\,(1/2)$ for the gg ($q\bar{q}$) final state. The strong coupling constant is evaluated at scales $\beta_{\tilde{g}} m_{\tilde{g}}$. This corresponds to averaging over the annihilating states, which produces a smaller correction than summing up all the contributions. We also neglect the possibility of gluinos forming bound states, which would further enhance gluino annihiliations (often quite dramatically). Therefore, our assumption about including the nonperturbative effects in the gluino annihilations ensures that the NLSP relic density calculated here is at worst an upper bound, so the claim that a given model satisfies the BBN bound is robust [62].

We can now calculate the final NLSP abundance from:

$$Y_{\rm NLSP} = \frac{1}{\int_{x_F}^{\infty}\sqrt{\frac{\pi g_*}{45}}\frac{mM_P}{x^2}\langle\sigma v\rangle\,{\rm d}x}\,, \quad (15)$$

which can be used to evaluate the standard cosmological parameter

$$\Omega_{\rm NLSP}h^2 = \frac{ms_0 Y_{\rm NLSP}}{\rho_c}\,, \quad (16)$$

where the present entropy density is $s_0 = 2889.2\,{\rm cm}^{-3}$ and the critical density is $\rho_c = 1.0539\cdot 10^{-5}\,{\rm GeV\,cm}^{-3}$.

[1] For a review, see, e.g., G. F. Giudice and R. Rattazzi, Phys. Rept. **322** (1999) 419 [arXiv:hep-ph/9801271].

[2] Z. Lalak, S. Pokorski and K. Turzynski, JHEP **0810** (2008) 016 [arXiv:0808.0470 [hep-ph]].

[3] K. Hamaguchi, E. Nakamura, S. Shirai and T. T. Yanagida, JHEP **1004** (2010) 119 [arXiv:0912.1683 [hep-ph]].

[4] A. Boyarsky, J. Lesgourgues, O. Ruchayskiy and M. Viel, JCAP **0905** (2009) 012 [arXiv:0812.0010 [astro-ph]].

[5] M. Bolz, A. Brandenburg and W. Buchmuller, Nucl. Phys. B **606** (2001) 518 [Erratum-ibid. B **790** (2008) 336] [arXiv:hep-ph/0012052].

[6] J. Pradler and F. D. Steffen, Phys. Rev. D **75** (2007) 023509 [arXiv:hep-ph/0608344].

[7] V. S. Rychkov and A. Strumia, Phys. Rev. D **75** (2007) 075011 [arXiv:hep-ph/0701104].

[8] M. Olechowski, S. Pokorski, K. Turzynski and J. D. Wells, JHEP **0912** (2009) 026 [arXiv:0908.2502 [hep-ph]].

[9] K. Jedamzik, M. Lemoine and G. Moultaka, JCAP **0607** (2006) 010 [arXiv:astro-ph/0508141].

[10] M. Kawasaki, F. Takahashi and T. T. Yanagida, Phys. Lett. B **638** (2006) 8 [arXiv:hep-ph/0603265].

[11] R. Allahverdi, A. Jokinen and A. Mazumdar, Phys. Rev. D **71** (2005) 043505 [arXiv:hep-ph/0410169].

[12] S. Davidson, E. Nardi and Y. Nir, Phys. Rept. **466** (2008) 105 [arXiv:0802.2962 [hep-ph]].

[13] S. Antusch and A. M. Teixeira, JCAP **0702** (2007) 024 [arXiv:hep-ph/0611232].

[14] S. Davidson, J. Garayoa, F. Palorini and N. Rius, JHEP **0809** (2008) 053 [arXiv:0806.2832 [hep-ph]].

[15] G. F. Giudice, A. Notari, M. Raidal, A. Riotto and A. Strumia, Nucl. Phys. B **685** (2004) 89 [arXiv:hep-ph/0310123].

[16] A. Anisimov, W. Buchmuller, M. Drewes and S. Mendizabal, Phys. Rev. Lett. **104** (2010) 121102 [arXiv:1001.3856 [Unknown]].

[17] M. Flanz, E. A. Paschos and U. Sarkar, Phys. Lett. B **345** (1995) 248 [Erratum-ibid. B **382** (1996) 447] [arXiv:hep-ph/9411366].

[18] K. Turzynski, Phys. Lett. B **589** (2004) 135 [arXiv:hep-ph/0401219].

[19] T. Hambye, Y. Lin, A. Notari, M. Papucci and A. Strumia, Nucl. Phys. B **695** (2004) 169 [arXiv:hep-ph/0312203].

[20] M. Raidal, A. Strumia and K. Turzynski, Phys. Lett. B **609** (2005) 351 [Erratum-ibid. B **632** (2006) 752] [arXiv:hep-ph/0408015].

[21] H. Murayama and T. Yanagida, Phys. Lett. B **322** (1994) 349 [arXiv:hep-ph/9310297].

[22] G. F. Giudice, L. Mether, A. Riotto and F. Riva, Phys. Lett. B **664** (2008) 21 [arXiv:0804.0166 [hep-ph]].

[23] Y. Grossman, T. Kashti, Y. Nir and E. Roulet, Phys. Rev. Lett. **91** (2003) 251801 [arXiv:hep-ph/0307081].

[24] G. D'Ambrosio, G. F. Giudice and M. Raidal, Phys. Lett. B **575** (2003) 75 [arXiv:hep-ph/0308031].

[25] K. Hamaguchi and N. Yokozaki, arXiv:1007.3323 [hep-ph].

[26] E. Komatsu *et al.* [WMAP Collaboration], Astrophys. J. Suppl. **180** (2009) 330 [arXiv:0803.0547 [astro-ph]].

[27] J. R. Ellis, D. V. Nanopoulos and S. Sarkar, Nucl. Phys. B **259** (1985) 175.

[28] F. Balestra *et al.*, Nuovo Cim. A **92** (1986) 139.

[29] M. Kawasaki and T. Moroi, Prog. Theor. Phys. **93** (1995) 879 [arXiv:hep-ph/9403364].

[30] J. R. Ellis, D. V. Nanopoulos, K. A. Olive and S. J. Rey, Astropart. Phys. **4** (1996) 371 [arXiv:hep-ph/9505438].

[31] J. R. Ellis, K. A. Olive, Y. Santoso and V. C. Spanos, Phys. Lett. B **588** (2004) 7 [arXiv:hep-ph/0312262].

[32] M. Kawasaki, K. Kohri and T. Moroi, Phys. Rev. D **71**, 083502 (2005) [arXiv:astro-ph/0408426].

[33] J. L. Feng, S. f. Su and F. Takayama, Phys. Rev. D **70** (2004) 063514 [arXiv:hep-ph/0404198].

[34] J. L. Feng, S. Su and F. Takayama, Phys. Rev. D **70** (2004) 075019 [arXiv:hep-ph/0404231].

[35] L. Roszkowski, R. Ruiz de Austri and K. Y. Choi, JHEP **0508** (2005) 080 [arXiv:hep-ph/0408227].

[36] D. G. Cerdeno, K. Y. Choi, K. Jedamzik, L. Roszkowski and R. Ruiz de Austri, JCAP **0606** (2006) 005 [arXiv:hep-ph/0509275].

[37] K. Jedamzik, Phys. Rev. D **74** (2006) 103509 [arXiv:hep-ph/0604251].

[38] K. Jedamzik, JCAP **0803**, 008 (2008) [arXiv:0710.5153 [hep-ph]].

[39] S. Dimopoulos, D. Eichler, R. Esmailzadeh and G. D. Starkman, Phys. Rev. D **41** (1990) 2388.

[40] M. Pospelov, Phys. Rev. Lett. **98** (2007) 231301 [arXiv:hep-ph/0605215].

[41] J. Pradler and F. D. Steffen, Phys. Lett. B **666** (2008) 181 [arXiv:0710.2213 [hep-ph]].

[42] J. Pradler and F. D. Steffen, Phys. Lett. B **648** (2007) 224 [arXiv:hep-ph/0612291].

[43] K. Y. Choi, L. Roszkowski and R. Ruiz de Austri, JHEP **0804** (2008) 016 [arXiv:0710.3349 [hep-ph]].

[44] F. D. Steffen, Phys. Lett. B **669** (2008) 74 [arXiv:0806.3266 [hep-ph]].

[45] D. G. Cerdeno, Y. Mambrini and A. Romagnoni, JHEP **0911** (2009) 113 [arXiv:0907.4985 [hep-ph]].

[46] J. Pradler and F. D. Steffen, Nucl. Phys. B **809** (2009) 318 [arXiv:0808.2462 [hep-ph]].

[47] L. Covi, J. Hasenkamp, S. Pokorski and J. Roberts, JHEP **0911** (2009) 003 [arXiv:0908.3399 [hep-ph]].

[48] J. Hasenkamp and J. Kersten, arXiv:1008.1740 [hep-ph].

[49] L. Boubekeur, K. Y. Choi, R. R. de Austri and O. Vives, arXiv:1002.0340 [Unknown].

[50] S. Bailly, K. Y. Choi, K. Jedamzik and L. Roszkowski, JHEP **0905** (2009) 103 [arXiv:0903.3974 [hep-ph]].

[51] M. Ratz, K. Schmidt-Hoberg and M. W. Winkler, JCAP **0810** (2008) 026 [arXiv:0808.0829 [hep-ph]].

[52] T. Kanzaki, M. Kawasaki, K. Kohri and T. Moroi, Phys. Rev. D **76** (2007) 105017 [arXiv:0705.1200 [hep-ph]].

[53] M. Kawasaki, K. Kohri, T. Moroi and A. Yotsuyanagi, Phys. Rev. D **78** (2008) 065011 [arXiv:0804.3745 [hep-ph]].

[54] W. Buchmuller, L. Covi, J. Kersten and K. Schmidt-Hoberg, JCAP **0611** (2006) 007 [arXiv:hep-ph/0609142].

[55] L. Covi and S. Kraml, JHEP **0708** (2007) 015 [arXiv:hep-ph/0703130].

[56] J. R. Ellis, K. A. Olive and Y. Santoso, JHEP **0810** (2008) 005 [arXiv:0807.3736 [hep-ph]].

[57] G. Belanger, F. Boudjema, A. Pukhov and A. Semenov, Comput. Phys. Commun. **176** (2007) 367 [arXiv:hep-

ph/0607059].
[58] G. Belanger, F. Boudjema, A. Pukhov and A. Semenov, Comput. Phys. Commun. **180** (2009) 747 [arXiv:0803.2360 [hep-ph]].
[59] L. Randall, R. Sundrum, Nucl. Phys. **B557**, 79-118 (1999). [hep-th/9810155].
[60] G. F. Giudice, M. A. Luty, H. Murayama, R. Rattazzi, JHEP **9812**, 027 (1998). [hep-ph/9810442].
[61] M. Kusakabe, T. Kajino, T. Yoshida and G. J. Mathews, Phys. Rev. D **80** (2009) 103501 [arXiv:0906.3516 [hep-ph]].
[62] C. F. Berger, L. Covi, S. Kraml and F. Palorini, JCAP **0810** (2008) 005 [arXiv:0807.0211 [hep-ph]].
[63] J. Alwall *et al.*, JHEP **0709**, 028 (2007) [arXiv:0706.2334 [hep-ph]].
[64] We wish to thank H. Flaecher for discussions on triggers and analysis criteria at the LHC.
[65] For a recent example, see G. F. Giudice, T. Han, K. Wang and L. T. Wang, Phys. Rev. D **81**, 115011 (2010) [arXiv:1004.4902 [hep-ph]].
[66] J. Alwall, M. P. Le, M. Lisanti and J. G. Wacker, Phys. Rev. D **79**, 015005 (2009) [arXiv:0809.3264 [hep-ph]].
[67] CMS Collaboration, "Search for Mono-jet Final States from ADD Extra Dimensions," CMS PAS EXO-08-011 (7 August 2009).
[68] L. Vacavant and I. Hinchliffe, J. Phys. G **27**, 1839 (2001).
[69] T. G. Rizzo, Phys. Lett. B **665**, 361 (2008) [arXiv:0805.0281 [hep-ph]].
[70] K. Nakamura et al. (Particle Data Group), "Review of Particle Physics", J. Phys. G37, 075021 (2010).
[71] C. H. Chen, M. Drees, J. F. Gunion, Phys. Rev. **D55**, 330-347 (1997). [hep-ph/9607421].
[72] J. F. Gunion, S. Mrenna, Phys. Rev. **D62**, 015002 (2000). [hep-ph/9906270].
[73] M. Fujii, M. Ibe and T. Yanagida, Phys. Lett. B **579** (2004) 6 [arXiv:hep-ph/0310142].
[74] H. Baer, K. m. Cheung and J. F. Gunion, Phys. Rev. D **59** (1999) 075002 [arXiv:hep-ph/9806361].
[75] D. Feldman, Z. Liu and P. Nath, Phys. Rev. D **80** (2009) 015007 [arXiv:0905.1148 [hep-ph]].